Progression of Elevated Temperatures in Municipal Solid Waste Landfills

Navid H. Jafari, A.M.ASCE[1]; Timothy D. Stark, F.ASCE[2]; and Todd Thalhamer[3]

Abstract: Elevated temperatures in municipal solid waste landfills can pose health, environmental, and safety risks because they can generate excessive gases, liquids, pressures, and heat that can damage landfill infrastructure. This paper discusses mechanisms that can lead to elevated temperatures in the landfill and presents a case history to establish trends in gas composition, leachate collection, settlement, and slope movement. In general, landfill gas composition changes from predominantly methane [50–60% volume-to-volume ratio (v/v)] and carbon dioxide (40–55% v/v) to a composition of carbon dioxide (60–80% v/v), hydrogen (10–35% v/v), and carbon monoxide [>1,500 parts per million per volume (ppmv)] as temperatures elevate. As waste temperatures increase, gas and leachate pressures also increase, resulting in odors, leachate outbreaks, and potential slope instability. These observations are summarized in a progression of elevated temperature indicators that are related to field manifestations and possible remedial measures. Finally, biological and chemical processes are proposed to explain the changes in internal landfill processes. **DOI: 10.1061/(ASCE)GT.1943-5606.0001683.** *© 2017 American Society of Civil Engineers.*

Author keywords: Landfill; Municipal solid waste; Smoldering combustion; Fire; Rapid oxidation; Pyrolysis; Temperature.

Introduction

Elevated landfill temperature events (ETLEs) have been documented in municipal solid waste (MSW) landfills, construction demolition debris landfills, industrial waste fills, and sanitary dumps (Martin et al. 2013; Sperling and Henderson 2001; Hogland and Marques 2003; Ettala et al. 1996; Riquier et al. 2003; Øygard et al. 2005; El-Fadel et al. 1997; Nikolaou 2008; Merry et al. 2005; Koelsch et al. 2005; Frid et al. 2010). The presence of ETLEs can impact the integrity of the landfill cover and liner systems, leachate quality, gas composition, slope stability, differential settlement, odor mitigation, and abatement operations (Lewicki 1999; Øygard et al. 2005; Jafari et al. 2014b; Stark et al. 2012). If temperatures are high enough to initiate a smoldering event, i.e., the condition that results in thermal degradation of MSW, they present a significant threat to the environment by emitting incomplete combustion byproducts, dioxins and furans, reduced sulfur compounds, and particulate matter to the atmosphere (Nammari et al. 2004; Ruokojärvi et al. 1995; Lönnermark et al. 2008; Chrysikou et al. 2008). Specifically, emitted air pollutants include, but are not limited to, carbon monoxide, volatile organic compounds (VOCs) (e.g., benzene and methyl-ethyl ketone), polycyclic aromatic hydrocarbons (PAHs), and semivolatile organic compounds (SVOCs), each of which can pose safety and environmental health threats (Martin et al. 2013; Stark et al. 2012; Szczygielski 2007; Bates 2004; Nammari et al. 2004)

The definition of ETLEs varies among landfill owners, consultants, researchers, and regulators. In this study, the concept of ETLEs involves MSW temperatures increasing above a threshold, which begins to stress the biochemical decomposition processes, engineered barriers, and gas collection and leachate removal systems. Municipal solid waste landfills with a gas collection and control system in accordance with federal regulations (40 CFR § 60.753) are required to operate each gas extraction well with a gas wellhead temperature less than 55°C (131°F), which is part of the New Source Performance Standards (NSPS) established by Clean Air Act Amendments of 1970 (42 U.S.C. § 7401 et seq.). Based on landfill gas wellhead monitoring, temperatures in MSW landfills are usually within the mesophilic range of 38–54°C (Emcon Associates 1981; Yesiller et al. 2005; Houi et al. 1997). Specifically, the mesophilic bacteria that regulate methane generation occur best at approximately 40°C (Hartz et al. 1982; Cecchi et al. 1993; Mata Àlvarez and Martínez Viturtia 1986; Pfeffer 1974), while thermophilic methanogens have a temperature optimum of approximately 65°C, with 70°C as an approximate upper limit for acetate conversion to methane (Zinder 1993). Although there is not a simple upper temperature limit for methanogens, laboratory reactors simulating anaerobic decomposition of MSW indicate that methane production starts to decrease significantly if waste temperature exceeds 55°C (Kasali and Senior 1989; Hartz et al. 1982). This decrease is attributed to the mesophilic bacteria population being significantly reduced (Farquhar and Rovers 1973; McBean et al. 1995). Therefore, this paper considers elevated temperatures in MSW landfills as gas wellhead temperatures above 65°C, i.e., temperatures above which anaerobic biodegradation is usually curtailed.

To rapidly detect ETLEs, landfill operators, consultants, and regulatory agencies have used infrared imagery, geophysical (electric and electromagnetic) techniques, visual observations (surface settlement, smoke, and steam), and monitoring of waste temperatures, gas composition and temperature, and leachate quality (Stearns and Petoyan 1984; Lewicki 1999; Riquier et al. 2003;

[1]Assistant Professor, Dept. of Civil and Environmental Engineering, Louisiana State Univ., 3316 N Patrick Taylor Hall, Baton Rouge, LA 70803 (corresponding author). E-mail: njafari@lsu.edu

[2]Professor, Dept. of Civil and Environmental Engineering, Univ. of Illinois, 205 N. Mathews Ave., Urbana, IL 61801-2352. E-mail: tstark@illinois.edu

[3]Civil Engineer, California Environmental Protection Agency, 1001 I St., Sacramento, CA 95812. E-mail: Todd.Thalhamer@CalRecycle.ca.gov

Note. This manuscript was submitted on August 20, 2016; approved on December 1, 2016; published online on March 23, 2017. Discussion period open until August 23, 2017; separate discussions must be submitted for individual papers. This paper is part of the ***Journal of Geotechnical and Geoenvironmental Engineering***, © ASCE, ISSN 1090-0241.

Sperling and Henderson 2001; Riviere et al. 2003; DMWM 2011; Copping et al. 2007). For instance, Stark et al. (2012) used a case study to illustrate gas and leachate as indicators for aluminum production waste (APW) reactions in a MSW facility. Building on Stark et al. (2012), Martin et al. (2013) provided operational criteria and landfill trends to determine if an APW reaction is occurring at a facility and to distinguish between an APW reaction and subsurface smoldering combustion. While techniques are readily available to detect elevated temperatures, the spatial and temporal variations of landfill gas, temperature, leachate migration, and settlement resulting from ETLEs are lacking. This paper presents a case history on elevated gas and waste temperatures, changes in gas composition and production, leachate migration, slope movement, and settlement to develop a progression of elevated temperature indicators. These indicators are linked to field manifestations and possible chemical mechanisms.

Causes of Elevated Landfill Temperatures

Several factors can lead to landfill temperatures exceeding 65°C, including aerobic decomposition, air intrusion, self-heating, partially extinguished surface fires, exothermic chemical reactions, spontaneous combustion, and smoldering combustion. Municipal solid waste landfills have experienced elevated temperatures due to exothermic chemical reactions of industrial wastes, including APW (Calder and Stark 2010), incinerator ash, landfilled hot wastes, bottom ash (Klein et al. 2001, 2003), tires (Wappett and Zornberg 2006), iron waste, steel mill slag, petroleum coke, flue gas desulfurization gypsum, fluidized bed combustion residues (Anthony et al. 1999), lime kiln dust, and dried wastewater sludge (Zerlottin et al. 2013). For example, the APW reaction involves the amphoteric reaction of metallic aluminum with water to produce hydrogen gas and heat (Calder and Stark 2010; Stark et al. 2012). Observed temperatures of MSW landfills undergoing aluminum reactions range from 88 to 110°C (Stark et al. 2012; Jafari et al. 2014a).

A common mechanism causing elevated temperatures is the introduction of ambient air into a landfill during gas collection and control operations. The typical vacuum applied for a gas extraction well is approximately 125–250 mm (5–10 in.) of water column (USACE 2008). When landfill operators further increase the vacuum to enhance methane recovery for energy production (i.e., overdrawing the gas collection system), oxygen can enter the landfill through damaged gas wellhead seals and cracks, cracks in the soil cover, poorly compacted cover soils and slopes, and unsaturated subsurface materials. Aerobic decomposition can start from these and other actions that allow oxygen to enter the waste, such as rapid settlement, poorly compacted or inadequate soil covers especially on side slopes, abandoned gravel access roads, uncapped borings, leachate sumps, drainage systems, and passive venting systems. Changes in atmospheric pressure from cold fronts can also move landfill gas out or air into a landfill body (Young 1992; Nastev et al. 2001; Ishigaki et al. 2005). In another condition, when higher temperature gases rise through the landfill, they are replaced with cooler incoming air from the side slopes. This chimney effect causes air to flow into the landfill, thus delivering oxygen into the waste body.

Municipal solid waste landfills undergo aerobic decomposition to produce carbon dioxide, water, and heat (Meraz and Domínguez 1998). As available oxygen is consumed, biological decomposition changes from aerobic to anaerobic with the resultant production of methane, carbon dioxide, and heat. Aerobic and anaerobic transformation of glucose as representative of the organic matter in the waste can be expressed by the reactions in Eqs. (1) and (2), respectively (Meraz and Domínguez 1998)

$$C_6H_{12}O_6\,(s) + 6\,O_2\,(g) \rightarrow 6\,CO_2\,(g) + 6\,H_2O\,(l) \qquad \Delta H = -2{,}815\ \mathrm{kJ/mol} \tag{1}$$

$$C_6H_{12}O_6\,(s) \rightarrow 3\,CO_2\,(g) + 3\,CH_4\,(g) \qquad \Delta H = -145\ \mathrm{kJ/mol} \tag{2}$$

Comparing the enthalpies of both reactions, heat generated in anaerobic decomposition is approximately 5% of the heat produced from the aerobic reaction (Meraz and Domínguez 1998). As a result, waste temperatures in aerobic conditions are in the range of 60–80°C (Haug 1997; Lefebvre et al. 2000; Merz and Stone 1970; Hudgins and Harper 1999), while anaerobic landfills typically have temperatures ranging from approximately 25–45°C (Yesiller et al. 2005; Hanson et al. 2010).

The introduction of oxygen in the waste mass and accumulation of heat via aerobic biodegradation or another exothermic process provides the necessary conditions to initiate and sustain subsurface combustion of MSW (Fire 1996). Based on the tetrahedron of combustion theory (Fire 1996), four conditions must be present for combustion to occur: (1) a fuel source, e.g., paper products in MSW; (2) an oxidizer, e.g., oxygen from air intrusion; (3) an energy source, e.g., heat generated from aerobic decomposition or other exothermic reaction; and (4) a self-sustaining chain reaction of combustion, e.g., charred waste. The fourth condition implies the released thermal energy from combustion feeds energy back into the system, allowing more MSW and oxygen to react, thus releasing more energy until the combustion is limited by the supply of fuel or oxygen. In this framework, aerobic decomposition contributes to two conditions (oxygen and initial energy source) that could lead to combustion. In MSW landfills, the reactant that can be readily controlled is air intrusion, so it is paramount to limit air intrusion and the spreading of combustion. Subsurface combustion typically propagates in landfills through smoldering combustion, which occurs directly on the surface of a solid fuel (Martin et al. 2013). Incomplete smoldering combustion of cellulose yields carbon dioxide, carbon monoxide, water vapor, and heat (Huggett 1980), as shown in the reaction in Eq. (3)

$$C_6H_{10}O_5\,(s) + 5.7O_2 \rightarrow 5.4\,CO_2\,(g) + 0.6\,CO\,(g) + 5H_2O \qquad \Delta H = -2{,}440\ \mathrm{kJ/mol} \tag{3}$$

Smoldering combustion does not proceed to completion because the amount of oxygen available is generally limited, but it can still propagate at low oxygen levels, e.g., <3% volume-to-volume ratio (v/v) (De Haan 2006; Pitts 2007). Smoldering combustion has been documented to persist within a MSW landfill between 100 and 120°C (Ettala et al. 1996). In other cases, smoldering combustion temperatures observed in MSW landfills have ranged from 200 to 300°C and as high as 700°C (Lönnermark et al. 2008; Ruokojärvi et al. 1995). Bergström and Björner (1992) measured temperatures of 80–230°C for a deep subsurface fire. As a result of smoldering combustion, waste temperatures can rise to sufficient levels to thermally degrade or char MSW.

Overview of Case Study

The case study presented herein is a MSW landfill regulated under Subtitle D of the Resource Conservation and Recovery Act (40 CFR § 258). The site is permitted for waste disposal in 178 ha

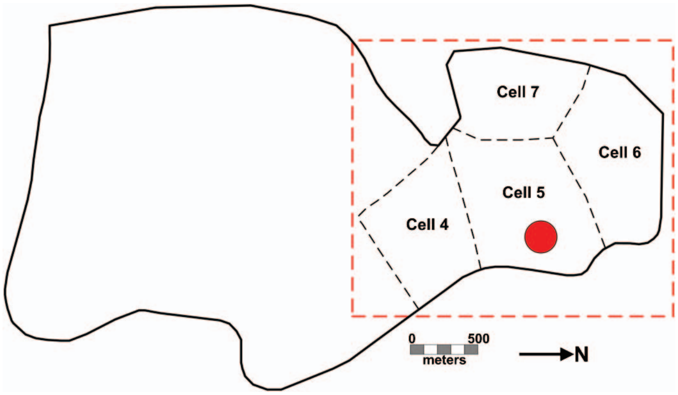

Fig. 1. (Color) Site layout of case study (dashed box is impacted area) with the red circle inside Cell 5 representing the estimated location of initial elevated temperatures

and receives up to 9,000 t of MSW per day. Fig. 1 shows the site layout and location of the impacted area in Cells 4–7 (dashed box). These cells encompass 26.2 ha and were constructed in phases, with Cell 4 completed in late 1997, Cell 5 in early 1999, Cell 6 in late 1999, and Cell 7 in early 2001. After reaching the permitted elevations in October 2005, Cells 4–7 were capped with a 0.6-m-thick fine-grained intermediate soil cover, and a gas control and collection system was installed.

In August 2009, five gas wellheads in Cell 5 experienced temperatures above 68°C and as high as 95°C (red circle in Fig. 1). Associated laboratory gas sampling from the wellheads reported carbon monoxide concentrations >1,000 parts per million per volume (ppmv), with a maximum of 10,200 ppmv. In response to the elevated temperatures, the facility reduced vacuums to the landfill gas wells in the impacted area, i.e., they allowed passive flow into the gas collection system. The facility suspended dewatering pumps inside the wellhead pipes, which were operated to increase the capture of methane gas for energy recovery. An additional 0.3 m of clayey soil cover was placed over a 4.8-ha area in Cell 5 to control odors. Elevated temperatures were first observed in Cell 5 and then migrated to Cells 6 and 7, with Cell 4 remaining mostly unaffected. In October 2009, the facility observed tension cracks at the crest of the Cell 5 slope and a month later toe bulging was observed at the bottom of the Cell 5 slope. Comparison of aerial topography of October 2008 and December 2009 indicated total settlement in excess of 6 m at the slope crest and approximately 1.2 m of upward movement at the toe of the Cell 5 slope. As a result, the facility constructed stability berms along the toe of the Cells 5 and 7 slopes. In October 2009, the facility began continuous surveying of the landfill, and settlement in the affected area had exceeded an additional 4 m by March 2010. Odor complaints by residents and commercial businesses increased from 121 in 2009 to 437 in 2010 and 566 in 2011. To reduce the odor nuisance, the facility initially installed a textured 1.5 mm (60-mil) high-density polyethylene (HDPE) geomembrane over Cell 5, increased flare capacity, immediately transported odorous leachate from the site, and operated stand-alone odor neutralizing systems. The exposed HDPE geomembrane was expanded in January 2012 to cover the entirety of Cells 5, 6, and 7 and a portion of Cell 4. In January 2013, the facility began replacing the HDPE geomembrane cover with a coextruded ethylene vinyl alcohol (EVOH) geomembrane because diffusion rates of VOCs through EVOH geomembranes are two to four orders of magnitude lower than through HDPE geomembranes (McWatters and Rowe 2015; Eun et al. 2014).

Based on the Findings and Orders, the facility initiated an expanded monitoring program to monitor and delineate the ETLE. This program included:

- Weekly measurements of gas wellhead temperature, flow rate, and pressure;
- Weekly measurements of fixed gases (methane, nitrogen, oxygen, hydrogen, carbon dioxide, and carbon monoxide) with a portable field gas chromatograph;
- Monthly topographic survey;
- Monthly measurement of stability pins (slope movement and elevation); and
- Weekly downhole temperature measurements in Cell 4.

Gas temperature, flow rate, and vacuum pressure were sampled at the gas port located on the wellhead (located above the surface) and recorded using the GEM2000 meter (LANDTEC, Dexter, Michigan). Fixed gases (CO_2, CH_4, N_2, O_2, H_2, and CO) were measured by a portable field gas chromatograph. Stability pins, i.e., a survey stake or hub, were anchored in the cover soil below the geomembrane cover and used to monitor changes in northing, easting, and elevation. The location of the pins below the geomembrane was determined using a magnetic survey. The change in elevation is compounded each month to determine the cumulative settlement. Downhole temperatures were obtained using Type T thermocouples covered in a protective sheath and installed in sand backfilled boreholes. The Type T thermocouples are rated for a temperature range of −185 to 315°C with an accuracy of ±0.5% + 1°C. The thermocouples were read by connecting the end clips to a Fluke 51 (FLUKE, Everett, Washington) or an equivalent single-input thermometer. Of the 25 thermocouples installed at this facility, 14 failed within 5 years. Specific causes of thermocouple failure are unknown but likely include wire corrosion from moisture, differential settlement, fluctuating resistance in the wires, calibration, and connectivity issues to the thermometer. Fig. 2(a) shows the location of gas extraction wells and stability pins used to correlate landfill trends. Fig. 2(b) shows the bottom liner system contour elevations, which are used to estimate the waste thicknesses in Fig. 2(c). Vertical strains were computed as the ratio of waste thickness at a specific time to the initial waste thickness, which was evaluated from Fig. 2(c) at each stability pin.

While this paper serves to illustrate the effect of ETLEs on changes in gas composition, leachate migration, settlement, and slope movement, the monitoring program was implemented by the landfill owner and regulatory agencies to define the nature, rate, and extent of the incident to assess public safety and mitigate environmental contamination. In other words, this monitoring program was not motivated by a research study, so the data collected are not all encompassing. For example, the extreme leachate and gas pressures during borehole drilling (directly affecting personnel safety) in Cell 5 prevented the possibility of obtaining waste temperatures in the epicenter of the elevated temperatures (red circle in Fig. 1). The landfill owner and regulatory agency did not further pursue this task because of many other site operation and maintenance commitments. In another case, the lack of historical leachate volumes and pumped leachate during the ETLE precluded the ability to perform a water balance analysis and evaluate if leachate volumes increased. This was attributed to the layout and operation of the leachate collection system, i.e., the total leachate volume was only evaluated for the entire site at the discharge point to the municipal sewer district. Only the number of hours a pump operated in the sumps in Cells 4–7 was recorded, but they could not be converted to volumes. Although this may limit the degree to which conclusions are substantiated, this monitoring program provides an excellent data set for an ETLE to develop and illustrate landfill behavior trends in the presence of elevated temperatures.

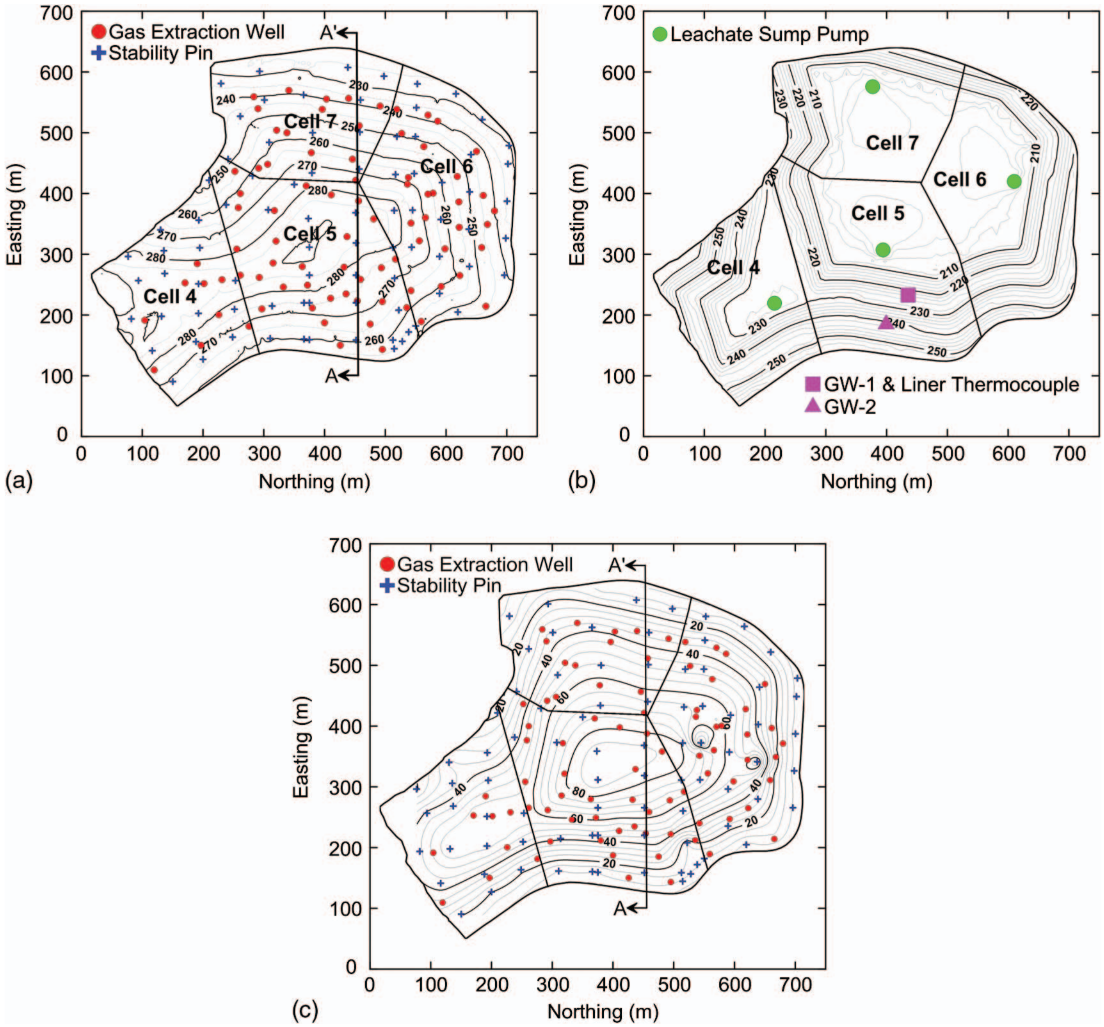

Fig. 2. (Color) Plan view of Cells 4–7 showing: (a) location of gas extraction wells and stability pins; (b) leachate and composite liner system elevations in meters; (c) waste thickness contours in meters

Measurement of Gas, Waste, and Bottom Liner Temperatures

One of the most important parameters used to assess whether or not a MSW landfill is operating normally is temperature (Hanson et al. 2010; Crutcher et al. 1982; Pfeffer 1974; Hartz et al. 1982). Landfill temperatures can be measured (1) at the gas wellhead, (2) using waste samples recovered during gas well drilling, and (3) with thermocouples installed at various depths in gas extraction well pipes, in boreholes, and in leachate collection pipes. Gas extraction wells collect gas from a slotted pipe, so temperatures represent an average over the slotted well pipe length and gas extraction well radius of influence. Temperatures of waste cuttings generated during drilling operations can be immediately measured by a thermal infrared camera. Downhole thermocouple arrays are more beneficial because they provide time-lapse in situ temperatures with depth.

An example of temperatures obtained using each method within Cell 4 is presented in Fig. 3. The gas extraction well was installed in 2005 to a depth of 33.2 m, where the lower 24.4 m consisted of slotted pipe. In October 2010, the landfill owner installed downhole thermocouple arrays to monitor waste temperatures in Cell 4. Boreholes were advanced using a 152-mm (6-in.) casing and drilled

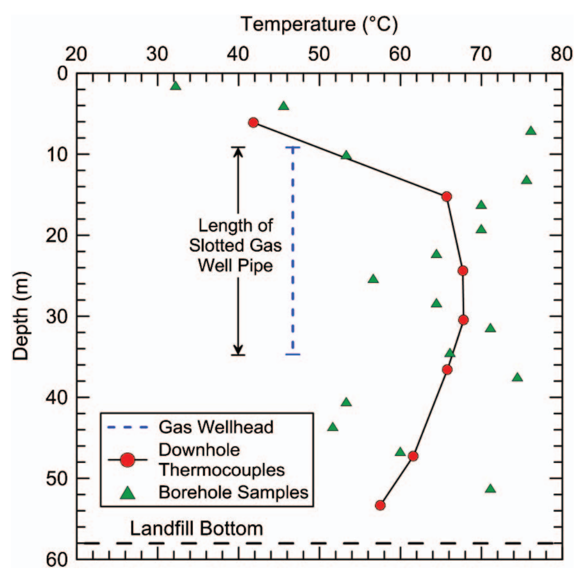

Fig. 3. (Color) Comparison of initial gas wellhead, waste sample, and downhole temperatures in Cell 4 with depth

with a 102-mm (4-in.) core barrel using the rotosonic drilling method. Seven Type T thermocouple sensors spaced 6.1–10.6 m apart were attached to a chlorinated polyvinyl chloride (CPVC) pipe and then lowered into the borehole. As the casing was removed, the borehole was backfilled with sand. The final 2.1 m to ground surface was backfilled with a 1.5-m bentonite plug and 0.6 m of cover soil. The waste samples recovered during drilling were immediately scanned with a thermal infrared camera. The gas wellhead, thermal infrared, and thermocouple measurements used in Fig. 3 were collected at the same time (mid-October 2010) and after the thermocouples had reached equilibrium with the surrounding waste. The gas wellhead temperature of 46°C is assumed to represent an average value over the screened depth because it precludes any contribution from deeper or shallower waste and the radius of influence of the wellhead. The thermocouple arrays measured a waste temperature of 42°C near the ground surface and a maximum temperature of 65°C within the middle one-third (depth 15–35 m) of the MSW. Downhole temperatures slightly decreased to 55°C near the landfill bottom (waste thickness is ~58 m). The thermal infrared temperatures suggest a similar trend with depth when compared with the thermocouples, but the values vary significantly due to likely heat loss during sample recovery.

Fig. 3 suggests that a thermal infrared camera can provide an approximate profile of waste temperature with depth and verify the initial thermocouple readings. For one-time sampling events, such as the thermal infrared camera, temperatures are less accurate because heat gain or loss may occur during drilling operations or during removal of samples from landfills. Gas wellhead temperatures in Fig. 3 are approximately 20°C lower than downhole temperatures because wellhead temperatures are influenced by mixing with surrounding gases in the wellhead and convective heat loss from waste to the ground surface (Martin et al. 2013). The slotted pipe also extends to approximately 55% of the waste thickness, so the gas extraction well may not show evidence of elevated temperatures because of the shallow pipe depth. The downhole temperature array in Fig. 3 located in Cell 4 is part of a system of sentinel wells that monitor movement of the ETLE toward Cell 4. These sentinel wells act as an early warning system for the landfill operator to install an isolation break, i.e., a physical barrier such as a vertical cutoff wall or an air gap created by excavating waste, to reduce the chance of the ETLE consuming a large portion of the facility. Fig. 4 shows the long-term temperature trend of the gas wellhead and downhole temperature array in Fig. 3. Specifically, in 2012, Fig. 4 shows that the maximum waste temperatures in Cell 4 are approximately 65°C from depths of 24.4 to 36.6 m. Temperatures at a depth of 6.1 m show fluctuations before an elapsed time of 900 days and after a time of 1,200 days. The cyclic variations may be caused by climatic factors or possible air intrusion that cools the MSW. Fig. 3 shows that the initial gas wellhead temperatures are 20°C lower than waste values in areas unaffected by elevated temperatures, and Fig. 4 corroborates this underprediction for a longer monitoring period.

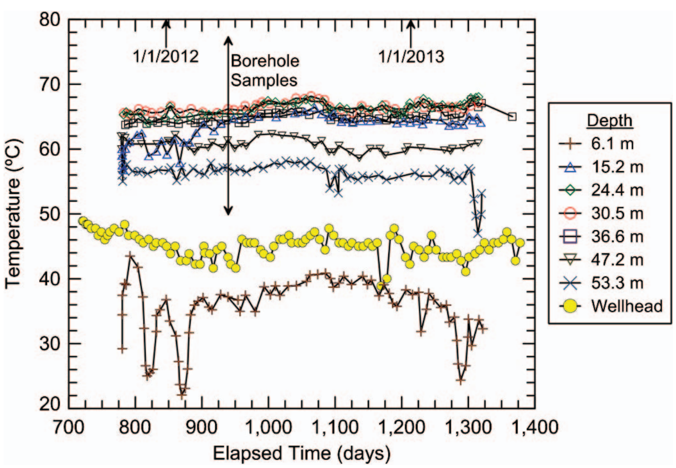

Fig. 4. (Color) Time lapse comparison of gas wellhead and downhole temperatures in Cell 4

Figs. 3 and 4 present wellhead and waste temperatures in Cell 4. They represent the initial or control conditions for Cells 5–7 prior to elevated temperatures developing at the gas extraction well. The landfill operators attempted to install downhole temperature arrays in Cell 5, but significant gas pressure prevented installation, which limited the available temperature data. To understand the progression of temperatures, Fig. 5 presents gas wellhead and bottom liner temperatures in Cell 5. The gas wellhead temperatures in Fig. 5(a) originate from GW-1 and GW-2 [Fig. 2(b) for locations], which are located near the ETLE epicenter. The bottom liner temperatures in Fig. 5(b) were measured using thermocouples inserted into the leachate collection system. In particular, a thermocouple was placed in the sump of Cell 5 while another thermocouple was installed approximately 120 m into the leachate collection pipe such that the final location was below GW-1. Gas temperatures in Fig. 5(a) initially start at ~90°C for GW-1, while GW-2 measures

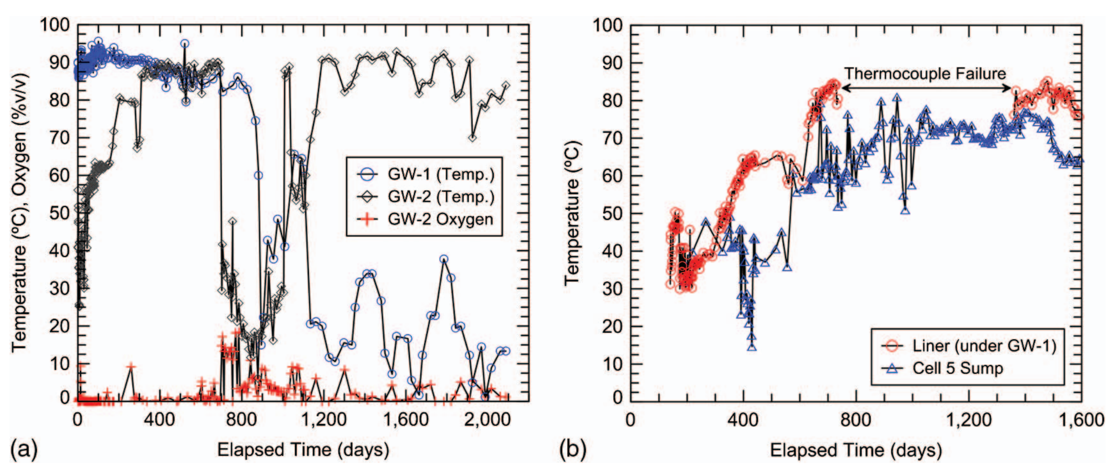

Fig. 5. (Color) Overview of Cell 5 temperatures from (a) gas wellheads; (b) thermocouples installed in the leachate collection system (note: different *x*-axis scales for both figures)

temperatures of 40°C and gradually increases to 90°C after an elapsed time of 350 days. Both gas wellheads maintain elevated temperatures until an elapsed time of 750 days, where they precipitously drop to approximately 20°C because of air intrusion into the wellhead. This observation is corroborated by oxygen levels of approximately 15% v/v measured in GW-2. Wellhead gas temperatures in GW-2 rebound and remain at approximately 90°C after oxygen levels subside. However, intermittent air intrusion into GW-1 likely resulted in the low, fluctuating temperatures after the initial air ingress. The behavior exhibited by GW-1 and similar wells in Cells 5–7 highlight the frequency of oxygen entering the landfill and the potential difficulty of obtaining representative gas wellhead temperatures in areas affected by elevated temperatures. In Fig. 5(b), bottom liner temperatures below GW-1 initially range from 30 to 50°C before they steadily increase to 85°C at an elapsed time of 700 days. Cell 5 sump temperatures increase suddenly from 40 to 63°C at a time of 575 days. The sump temperatures are approximately 5–10°C less than bottom liner temperatures because of the possible cooling effect from leachate and heat loss during pump operations. Because of thermocouple failure, bottom liner temperatures were unavailable under GW-1 from 750 to 1,350 days. However, the nearly constant Cell 5 sump temperatures suggest that GW-1 bottom liner temperatures also remained in the 80°C range. Although downhole measurements in Cell 5 are not available, the temperatures in Figs. 4 and 5 and observations from Martin et al. (2013), i.e., waste temperatures are 5–10°C greater than wellhead temperatures, suggest that waste temperatures in the impacted area of Cell 5 exceeded 100°C.

Changes in Landfill Gas Composition

Fig. 6 shows the relationship between increasing wellhead temperature and changes in the ratio of CH_4 to CO_2 gas, hydrogen levels, and carbon monoxide concentrations for a single gas extraction well in Cell 5. In terms of gas concentration, landfill gas is composed mostly of methane (45–60% v/v) and carbon dioxide (40–60% v/v) during anaerobic biodegradation, so a ratio of CH_4 to CO_2 close to unity provides a useful measure of microbial activity (Powell et al. 2006; Barlaz et al. 2010; Martin et al. 2013). The ratio of CH_4 to CO_2 was calculated by multiplying the volume-based concentration of CH_4 and CO_2 gases. Wellhead temperatures were measured at the gas wellhead using the gas analyzer GEM2000, while gas concentrations were measured by a portable field gas chromatograph.

In Fig. 6(a), the gas extraction well in Cell 5 is initially operating under normal conditions because wellhead temperatures are below the NSPS limit of 55°C and the ratio of CH_4 to CO_2 is greater than unity [Fig. 6(b)]. This represents the control conditions of the facility before initiation of elevated temperatures. The gas composition remains steady until an elapsed time of approximately 550 days when the ratio of CH_4 to CO_2 precipitously decreases from 1.2 to 0.3 in only 50 days ($t = 600$ days). Wellhead temperatures exceeded the NSPS threshold of 55°C at a time of 580 days, i.e., approximately a month after methane levels began decreasing, and gradually increased to 75°C at $t = 800$ days. A decreasing ratio of CH_4 to CO_2 before wellhead temperatures increase is a trend among several gas extraction wells at this facility. The delay before

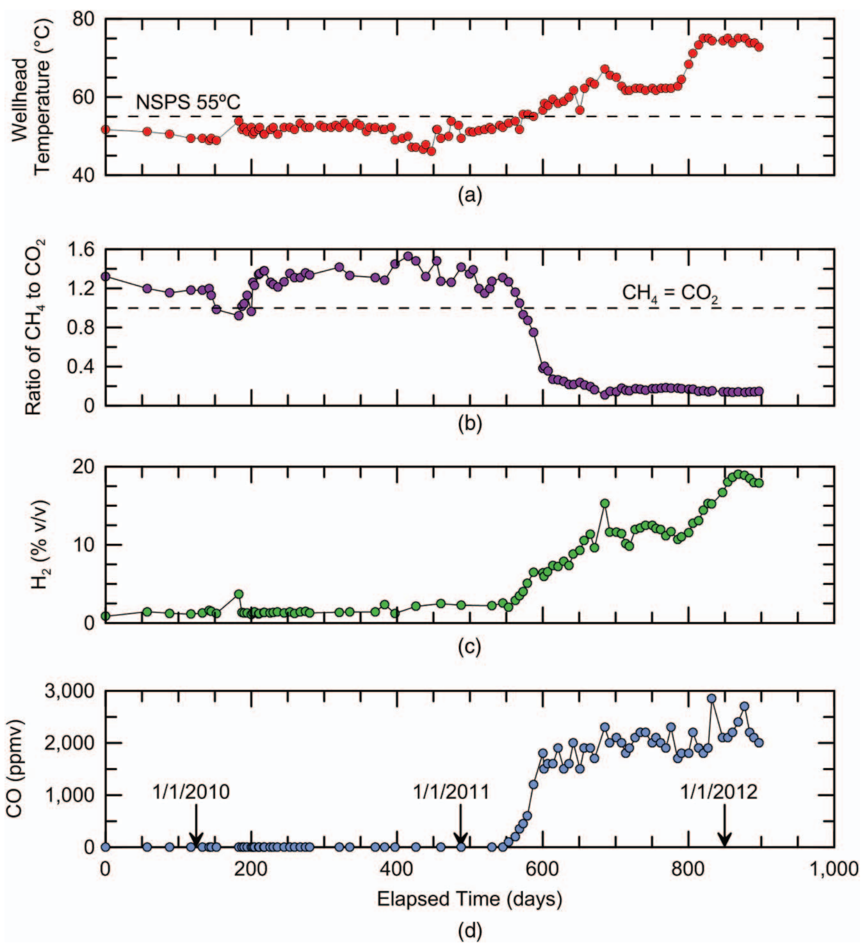

Fig. 6. (Color) Gas extraction well trends: (a) temperature; (b) ratio of CH_4 to CO_2; (c) hydrogen; (d) carbon monoxide

wellhead temperature increase may be attributed to the difference in gas flow and heat conduction through the waste. For example, heat conduction caused by only a thermal gradient is a slower process than convection of gas to an extraction well, so the increasing temperature trend occurs after the gas was removed. This observation suggests that changes in gas composition can occur in advance of the heating front (transition from anaerobic biodegradation gas indicators), with increasing wellhead temperatures being an indication of the approaching epicenter of ETLEs.

Hydrogen levels were <2% v/v and carbon monoxide (CO) was not measured when the ratios of CH_4 to CO_2 remained above unity. Fig. 6(c) shows that hydrogen increased at $t = 550$ days to a maximum concentration of 20% v/v. Similar to hydrogen, CO increased to ~1,800 ppmv at an elapsed time of $t = 550$ days, and remained in the range of 2,000–2,500 ppmv for the duration of the monitoring period. Combining the timeline in Figs. 6(b–d), it is evident that changes in the ratio of CH_4 to CO_2, hydrogen, and CO occur at the same time. Moreover, the ratio of CH_4 to CO_2 and CO are characterized by rapid changes, while hydrogen increase occurs at a slower pace, similar to wellhead temperature changes.

Elevated Gas and Leachate Pressures

Table 1 shows that MSW landfills under anaerobic biodegradation typically exhibit pressures up to 3 kPa. Stark et al. (2012) reported that installed piezometers in areas where APW reactions were occurring measured pressures up to 45 kPa. In addition, subsurface smoldering combustion can display significant gas pressures. For example, pressures of 25–45 kPa and as high as 75 kPa were observed in gas extraction wells at a facility in Illinois (Shaw Environmental 2008). In this case study, gas extraction wells located in the red circle in Fig. 1 also exhibited positive pressures, with maximum pressures reaching approximately 14 kPa.

Several mechanisms can contribute to increased gas pressures. Assuming a landfill is a constant volume boundary or sealed system (which may not be the case because of geomembrane cracking due to thermal elongation and differential settlement of waste), gas temperature and pressure increase simultaneously when considering the ideal gas law. For example, landfill gas is approximately atmospheric pressure (101.3 kPa) at a temperature of 40°C (Young 1992; Bogner et al. 1988). If subsurface temperatures increase to 100°C, internal gas pressures should increase by 19.4 kPa, thereby reducing the effective stress in the waste (about the same as 2 m of leachate). Convection can also drive hotter gases to the surface where they can accumulate under a geomembrane cover or emanate through the soil cover and result in odors. Furthermore, warmer gases carry a higher percentage of water vapor that can condense and clog the gas collection system wells and lateral headers. The clogged wells can reduce gas extraction capability, thus permitting subsurface pressures to increase even further. Similar to the APW reaction reported in Stark et al. (2012), elevated temperatures can

Table 1. Summary of Gas Pressures for Various Landfill Processes

Landfill process	Gas pressure (kPa)
Biodegradation[a]	0.5–3
APW reaction[b]	0.5–45+
Subsurface combustion[c]	5–75+

[a]Data from Bogner et al. (1988), Kerfoot (1993), Kjeldsen and Fischer (1995), Williams and Aitkenhead (1991), Wittman (1985), Nastev et al. (2001), and Young (1992).
[b]Data from Stark et al. (2012) and Martin et al. (2013).
[c]Current study.

initiate gas-generating processes, such as combustion and pyrolysis. The thermal breakdown of MSW into combustion ash yields approximately 30–50% by weight of char, 30–50% by weight of liquid, and 20–40% by weight of gas (Buah et al. 2007; Rampling and Hickey 1988; Williams and Besler 1993; Lin et al. 1999). This suggests elevated gas pressures can be explained by the increased gas production caused by combustion and pyrolysis. In conjunction with additional gas production, temperatures can damage and/or compromise gas extraction wells and lateral headers. Eventually, gas flow can exceed the capacity of the extraction well and header system, resulting in elevated gas pressures.

When gas and leachate migrate to landfill side slopes and are impeded by the cover system (soil and/or geomembrane), gas pressures and leachate can accumulate and cause leachate outbreaks. The elevated leachate and gas pressures occasionally manifest as leachate geysers that can eject 9–11 m into the air (Stark et al. 2012). These leachate geysers can also be encountered when borings are drilled in the waste for gas wells or exploratory purposes. In some instances where the soil cover system is replaced with a geomembrane to control odors, outbreaks can still occur at seams, gas wellhead connections, and geomembrane defects and whales even though the geomembrane encapsulates the surface.

Leachate and Moisture Migration

The convection of moisture-rich gas from dehydrated MSW can facilitate redistribution of leachate within the waste mass. When water vapor condenses, it can gravitate to the leachate collection system or accumulate in the gas extraction wells and header lines. For example, Stark et al. (2012) reported that a 35.7-ha facility generated between 3.8×10^6 and 23×10^6 L of leachate prior to an ETLE. After the ETLE began and expanded, leachate increased from 11.8×10^6 L in 2004 to 45.7×10^6 L in 2005 to 127×10^6 L in 2008, thus representing a sevenfold increase from the start of the ETLE. Given the elevated gas wellhead temperatures of 90°C in Fig. 5 and the fact that subsurface temperatures are higher (~20°C based on Fig. 3) than wellhead temperatures, sufficient heat is present to drive moisture from the MSW, where it can condense in gas extraction pipes and/or gravitate to one of the sumps. Increased leachate volume as reported by Stark et al. (2012) was not substantiated at this site because of the lack of leachate volume data. This precluded a water balance analysis to estimate the increase in moisture migration from dehydrated waste, while concomitantly evaluating the percolation of precipitation (limited because of the EVOH geomembrane liner) to the leachate drainage system. However, the facility does maintain records of the number of hours the leachate pumps located in Cells 4–7 are operated. They reported that the historical average pump usage for Cells 4–7 were 0.5, 0.8, 1.8, and 1.9 h/day. For the 4-year period of elevated temperatures, the average pump usage was 1.3, 5.6, 1.3, and 11.1 h/day for Cells 4–7, respectively. While only a qualitative assessment, the significant increase in pump usage for Cells 5 and 7 from historical values (i.e., by a factor of 7 and 5.8, respectively) suggests that the higher leachate collection rates are correlated to areas where the elevated temperatures caused the most settlement and slope movement, which are described in the next section.

Slope Movement and Settlement

Slope instability and movement has occurred at landfills with elevated temperature, leachate, and/or gas pressures (Stark et al. 2010, 2012; Koelsch et al. 2005; Jafari et al. 2013; Hendron et al. 1999; Blight 2008; Koerner and Soong 2000). The failure described

Fig. 7. (Color) Examples of (a) anaerobically decomposing waste sampled at a depth of 10.7 m (30 ft) (image courtesy of Ohio EPA); (b) thermally degraded (combusted) waste sampled at a depth of 25.9 m (85 ft) (image by Timothy D. Stark); both samples were approximately 15 years old and obtained from separate 100-mm-diameter rotosonic borings

by Stark et al. (2012) resulted in more than 6 m of displacement and waste moving outside of the permitted waste boundary. The shearing or tilting of vertical gas wellheads, tension cracks at or near the slope crest, and bulging of waste near the slope toe were indications of slope movement. Based on visual observations from this case study and two other elevated temperature sites, slope movement is preceded and accompanied by forceful gas and leachate outbreaks. Mechanisms for slope instability usually include elevated gas pressures, perched leachate surfaces, and/or reduced MSW shear strength (Stark et al. 2010). In particular, the interconnecting plastics and other reinforcing materials that contribute to the high shear strength of MSW are mostly consumed, charred, burnt, and/or decomposed at elevated temperatures. For example, Fig. 7(a) shows a sample of biologically decomposing waste where pieces of brown paper and plastic are still visible. In contrast, the elevated temperature sample shown in Fig. 7(b) is black and charred and resembles the texture of combustion ash. This comparison illustrates the physical change of MSW from biological to thermal decomposition, which can affect the shear strength and compressibility properties of the MSW.

Fig. 8 shows the cumulative slope movement and settlement obtained from stability pins installed beneath the geomembrane throughout Cells 4–7 [locations shown in Figs. 2(a and c)]. The northing, easting, and elevation of the pins were measured monthly to evaluate time-lapse slope movement and settlement. Surface movement is represented by vectors that show the direction and magnitude of movement. The vector angle is computed each month from the change in the northing and easting values, and the vector length is defined by the total distance travelled from the start of monitoring (September 2009).

In September 2010 [Fig. 8(a)] and after 1 year of elevated temperatures, cumulative settlement of approximately 4 m created a bowl-like shape feature in Cell 5. Two years after the onset of elevated temperatures [Fig. 8(b)], the settlement bowl depth increased to 6 m and width expanded radially into Cell 6. From September 2011 to February 2012, settlement increased significantly to 14 m. The settlement bowl extended into Cell 7 and approached the boundary of Cells 4 and 5 in February 2012. Cumulative settlement in the ETLE epicenter continued to rapidly increase through September 2012 and 2013. For example, Fig. 8(e) shows that ~20 m of settlement occurred in Cell 5. In the 4-year period from September 2009 to 2013, the average settlement rate in the bowl was 5 m/year. The initial waste height in Cell 5 was ~85 m, so the corresponding strain over the 4-year period was approximately 25%. During the 4 years of monitoring, the boundaries of the settlement bowl propagated into Cell 6 before advancing to Cell 7. More importantly, Fig. 8 indicates the settlement associated with elevated temperatures did not significantly affect Cell 4. The settlement within Cell 4 ranges between 0.25 and 2 m, with the upper bound likely attributed to the settlement in Cell 5, and signifies an average rate of only 0.06 to 0.5 m/year, respectively.

In September 2010 [Fig. 8(a)], the vectors in Cells 4, 6, and 7 are barely visible, i.e., slope movements are less than 0.15 m. However, vectors in Cell 5 (along cross section A–A′) indicate that approximately 2 m of cumulative slope movement has already occurred. In Cells 6 and 7 [Fig. 8(b)], the vectors are still small, i.e., less than 0.5 m, but it is evident they are pointing toward the landfill perimeter. The vector arrows in Cell 5 increased to approximately 4 m by September 2011, and they project in the direction of the Cell 5 slope because of the outward migration of the slope. After significant deepening of the settlement bowl by February 2012, the slope movement can be directly linked to the movement of the settlement bowl [Fig. 8(c)]. For example, the vectors projecting outward of Cell 5 are smaller in Fig. 8(c) because the epicenter of the settlement bowl settled sufficiently to drag the slope surface back toward the crater. The migration of the settlement bowl into Cell 7 shows vector arrows projecting out of Cell 7, with slope movements of approximately 2 m. This trend continues through September 2013. In Figs. 8(d and e), the vectors indicate the Cell 7 slope moved approximately 15 m.

Thus, Fig. 8 illustrates the dual nature or direction of slope movement. First, as the settlement bowl expands, gas and leachate pressures exert a force that pushes or bulges the slope outward. Second, if the settlement bowl continues to deepen, the slope movement can reverse directions, drift backward into the center of the elevated temperature zone, and subsequently produce a flatter slope. This explains why the vector arrows can increase and decrease in size with time and the vector angles can reverse direction. The comparison of slope movement and settlement in Fig. 8 shows that the ETLE starts in Cell 5 and expands significantly into Cells 6 and 7. The settlement bowl advances into Cell 6 and the vector arrows indicate cumulative slope movements of approximately 4 m, but Fig. 8 shows that the major thrust from elevated temperatures is primarily toward Cell 7.

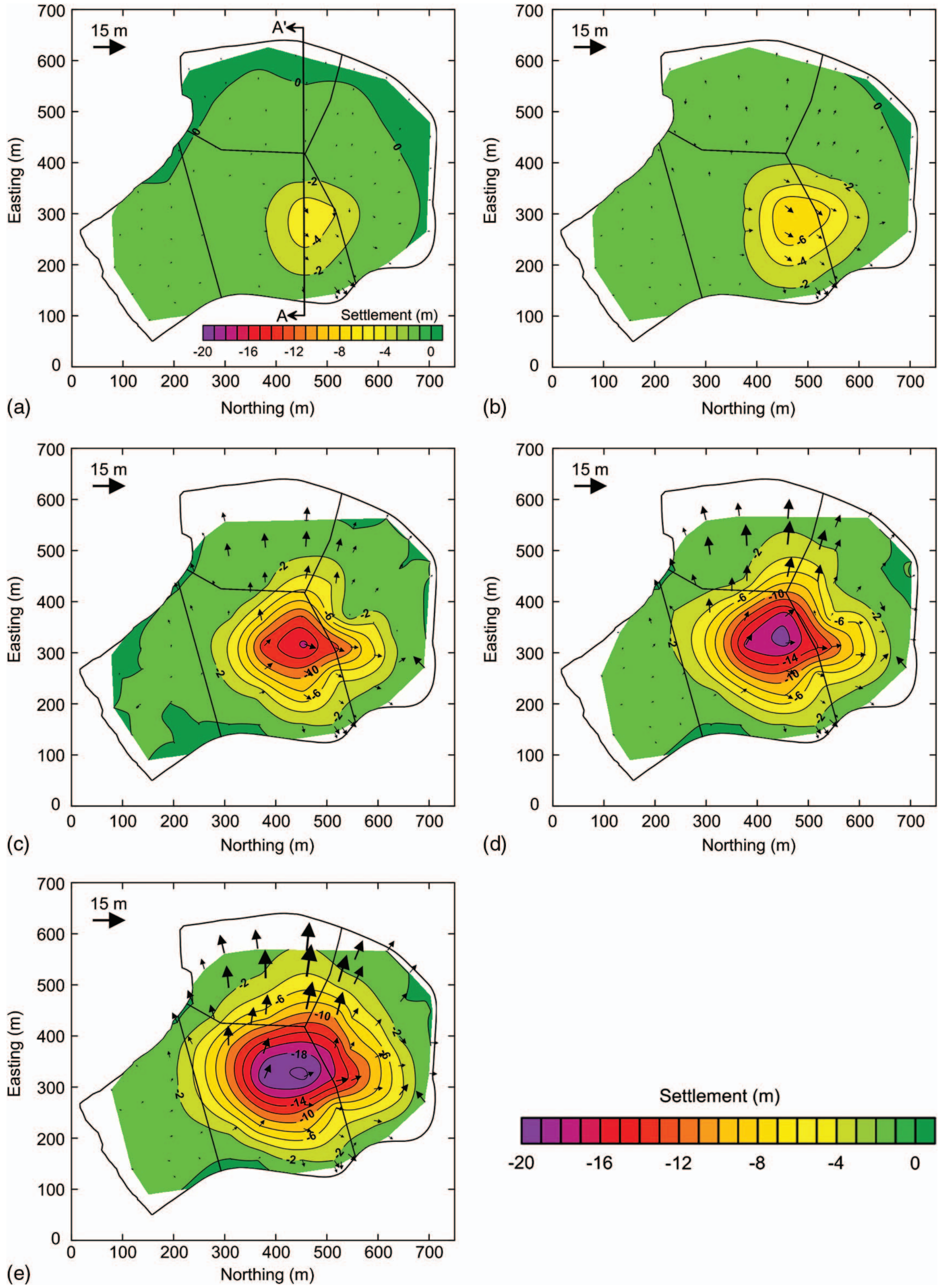

Fig. 8. (Color) Spatial expansion of settlement (meters; color contours) and corresponding slope movement (vectors) for (a) September 2010; (b) September 2011; (c) February 2012; (d) September 2012; (e) September 2013

Progression of Landfill Indicators

The preceding case study identifies the following landfill indicators after the onset of localized elevated waste temperatures: (1) concurrent changes in landfill gas composition and temperature, (2) measurable elevated gas and leachate pressures, (3) leachate migration, and (4) slope movement and/or settlement. After establishing the indicators, spatial and temporal relationships were investigated to arrange the landfill indicators in a chronological sequence. For example, cross section A-A′ in Fig. 2(a) extends from Cells 5 to 7, bisects the initial elevated temperature region, and is used to highlight when gas composition changes along a particular line of gas wells. The profile of cross section A-A′ and location of gas extraction wells B-1–B-6 are shown in Fig. 9. Furthermore, a stability pin

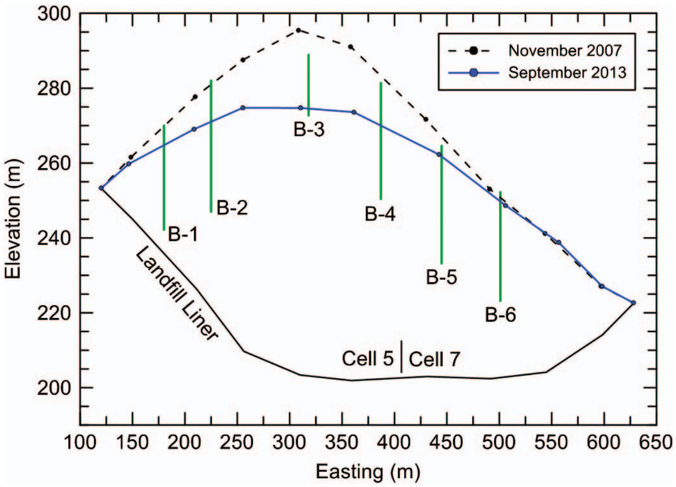

Fig. 9. (Color) Profile of cross section A-A′ showing gas extraction wells B-1–B-6 and landfill surface in November 2007 and September 2013

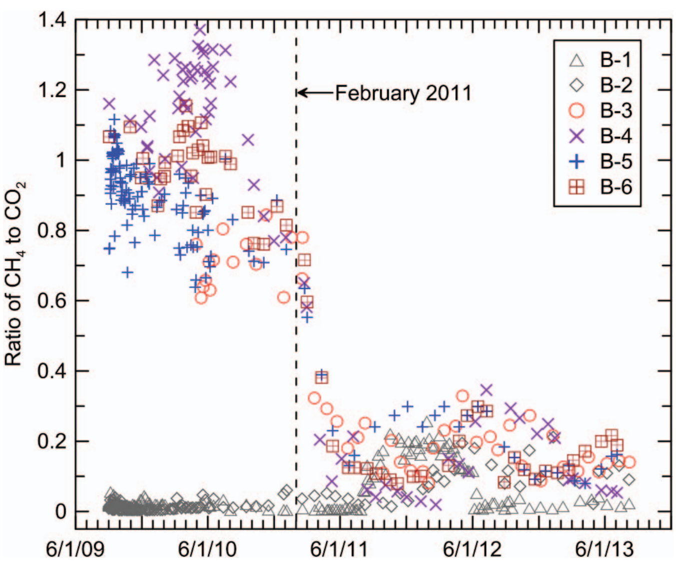

Fig. 10. (Color) Time lapse trend of ratio of CH_4 to CO_2 along cross section A-A′ for gas extraction wells B-1–B-6

and gas wellhead (located in Cell 5 and less than 3 m apart) provide a temporal comparison of settlement and gas composition, respectively, as they relate to trends exhibited by elevated temperatures.

Fig. 10 shows the trends in the ratio of CH_4 to CO_2 for gas extraction wells B-1–B-6 along cross section A-A′ (Fig. 9). Gas wells B-1 and B-2 are located within the initial elevated temperature zone in Cell 5, so the CH_4 to CO_2 ratio is approximately 0.1 in September 2009 and remains below 0.2 throughout the monitoring period. However, gas wells B-3 through B-6 are located outside of the immediate hot spot, and they show CH_4 to CO_2 ratio values near unity from September 2009 to December 2010, which indicates normal anaerobic decomposition. In February 2011, the ratio of CH_4 to CO_2 rapidly decreases in each well to values below 0.3. The decline in each well suggests that internal landfill processes changed simultaneously even though the distance from B-3 to B-6 is approximately 250 m. In other words, gas generated from the elevated temperature region is projecting in advance of the heat-generating region inside the landfill.

Similar to the gas extraction well in Fig. 6, Fig. 11 shows that the decline in CH_4 to CO_2 ratio is accompanied by increased CO and hydrogen levels. For example, Fig. 11(a) shows that CO concentrations begin to increase at a CH_4 to CO_2 ratio of 0.8. Carbon monoxide levels continue to increase from 500 to 8,000 ppmv for gas ratio values below 0.3. Fig. 11(b) shows that hydrogen levels are generally less than 8% v/v when the ratio of CH_4 to CO_2 is above unity. As this gas ratio decreases below 0.4, hydrogen levels continue to increase to approximately 36% v/v. Fig. 11(b) also suggests that hydrogen is present at CH_4 to CO_2 ratios above unity. However, the gas wellheads in Cell 4, which were not affected by elevated temperatures, show no evidence of hydrogen gas. This indicates that the presence of hydrogen, e.g., >1% v/v, when the ratio of CH_4 to CO_2 is above unity is a deviation of normal biodegradation pathways in MSW. The hydrogen concentrations of 8% v/v in Fig. 11(b) are likely attributed to mixing of landfill gases from nearby elevated temperature and biodegradation areas, and hydrogen concentrations of approximately 35% v/v at low ratios of CH_4 to CO_2 in gas extraction wells B-3–B-6 are mainly a consequence of elevated temperatures. Based on Figs. 11 and 12, landfill gas composition changes across the landfill to primarily carbon dioxide (60–80% v/v), hydrogen (10–35% v/v), and carbon monoxide (>1,500 ppmv) as the ETLE moves through the waste.

Fig. 12 shows the cumulative settlement of two stability pins. One pin is located in Cell 5 and subjected to elevated temperatures, while the other pin is in Cell 4, where normal anaerobic biodegradation prevails. The biodegradation pin shows that settlement

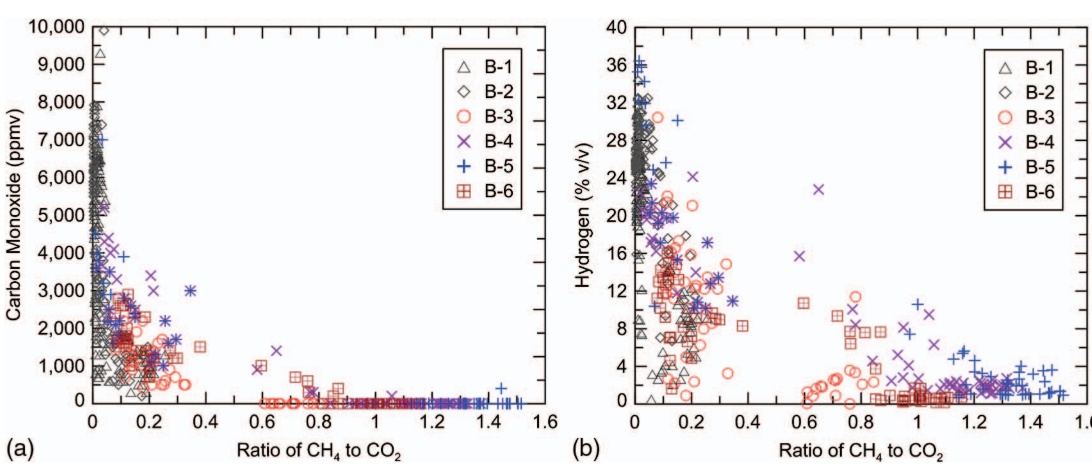

Fig. 11. (Color) Ratio of CH_4 to CO_2 in gas wells with (a) carbon monoxide; (b) hydrogen

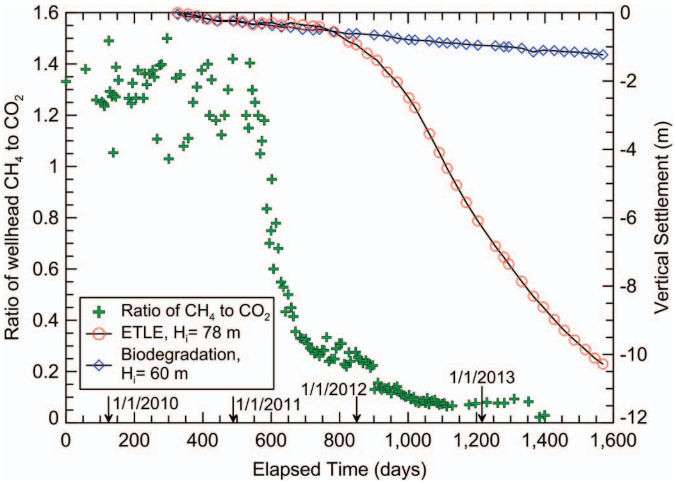

Fig. 12. (Color) Time-lapse comparison of ETLE and biodegradation settlement with decreasing ratio of CH_4 to CO_2

for a 60-m-thick waste area is only approximately 1.3 m in ~1,300 days, which corresponds to a strain rate of approximately 0.6%/year. The Cell 5 pin initially settles at the same rate as the biodegradation pin. However, settlement accelerates as the influence of elevated temperatures expand toward the stability pin. For example, vertical settlement is 0.5 m at an elapsed time of 800 days. By the end of the monitoring period, settlement is slightly over 10 m at $t = 1{,}600$ days. The corresponding strain rate of 5.7%/year is approximately 9.5 times greater than that provided by biodegradation alone, which is used herein as the control strain rate at this site. Fig. 12 also compares settlement with the ratio of CH_4 to CO_2 obtained from a gas extraction well located in the immediate vicinity of the Cell 5 pin. The ratio of CH_4 to CO_2 is above unity until time $t = 600$ days, after which it declines to a ratio of ~0.35 in 50 days. The ratio gradually decreases to ~0.1 after $t = 1{,}150$ days. Before settlement transitions from normal biodegradation to an accelerated rate, the ratio of CH_4 to CO_2 decreased to values that indicate anaerobic processes are inhibited. Thus, Fig. 12 shows that rapid settlement occurs after carbon dioxide concentration increases and is a delayed indicator of ETLEs. During the time gap of approximately 200 days in which landfill gas is rapidly changing composition, field observations indicate gas and leachate pressure increase and migration are contributing to slope movement before the onset of excessive settlement.

As a result, this case study shows that the initiation and expansion of elevated temperature results in a sequence of indicators that delineates the location, boundary, and movement. These indicators follow the systematic progression as follows: (1) changes in landfill gas composition, which are characterized by decreasing ratio of CH_4 to CO_2 and elevated carbon monoxide and hydrogen levels (gas composition is found to advance in front of the elevated temperature and heat-generating region); (2) increased odors; (3) elevated waste and gas temperatures, e.g., wellhead temperatures increased from below the NSPS threshold of 55–90°C; (4) elevated gas pressures and leachate migration that cause leachate outbreaks; (5) slope movement; and (6) unusual and rapid settlement.

Mechanisms Causing Landfill Inidicators

Rapid and Unusual Settlement

The last major consequence of elevated temperatures is excessive MSW settlement. The possible settlement mechanisms during elevated temperatures are moisture loss, thermal degradation, and mechanical creep. Biocompression, i.e., compression of the waste in response to biochemical processes that decompose the organic fraction (Bareither et al. 2012a), is not considered because anaerobic decomposition is inhibited by the elevated temperatures [the low methane concentrations in Figs. 6(b), 10, and 12]. Mechanical creep is the physical compression process in which void volume decreases with time as individual waste constituents yield under stress and slippage occurs at particle contacts (Bareither et al. 2012a). The vertical strain from mechanical creep can be estimated using the long-term C'_α settlement model (Bjarngard and Edgers 1990; Hossain and Gabr 2005; Bareither et al. 2012a)

$$\frac{\Delta H}{H} = C'_{\alpha M} \log\left(\frac{t_M < t < t_B}{t_M}\right) + C'_{\alpha B} \log\left(\frac{t_B < t < t_F}{t_B}\right) + C'_{\alpha MF} \log\left(\frac{t_F < t}{t_F}\right) \tag{4}$$

where ΔH = settlement (m); H = initial waste thickness (~78 m); $C'_{\alpha M}$ = mechanical creep ratio; $C'_{\alpha B}$ = biocompression ratio, t_M = transition time from immediate compaction to mechanical creep; t_B = time where settlement transitions from mechanical creep to biocompression; t_F = time where settlement is governed by final mechanical creep; and t = elapsed time since waste placement. The first term on the right side of Eq. (4) is used to evaluate the contribution of mechanical creep during the period of rapid settlement in Fig. 12. The elapsed times t_M and t_B were determined by assuming the time of waste placement in Cell 5 was October 2005 ($t = 0$ days) and then correlating t_B and t_M to the duration of accelerated settlement in Fig. 12. In this framework, elapsed times of 800 and 1,600 days in Fig. 12 correspond to t_M and t_B of 2,185 and 2,985 days, respectively. Bareither et al. (2012b) reported a range of $C'_{\alpha M}$ from 0.04 to 0.07 measured from a field-scale lysimeter experiment. Assuming an average $C'_{\alpha M} = 0.05$, the upper bound contribution of mechanical creep is approximately 0.55 m, which suggests mechanical creep was not a significant contributor to the observed rapid settlement. An inverse analysis of Fig. 12 for the ETLE pin indicates that $C'_{\alpha T}$ (thermal degradation compression ratio) is approximately 0.9.

The stability pins in Cells 4 and 5 in Fig. 12 also provide an opportunity to determine field values of C'_α representing mechanical creep and biocompression for a landfill in which leachate was not recirculated. The value of t_M was assumed to be 1,715 days ($t = 330$ days in Fig. 12, which reflects the start of available data), with t_B equal to 2,185 days ($t = 800$ days in Fig. 12) and 2,985 days ($t = 1{,}600$ days in Fig. 12) for Cells 5 and 4, respectively. Based on the magnitude of settlement shown in Fig. 12, the resulting C'_α is 0.087 and 0.061 for Cells 4 and 5, respectively. These low values of C'_α suggest that the predominant mechanism of settlement in this facility is mechanical creep and to a lesser extent biocompression because $C'_{\alpha B}$ values obtained from large-scale test cells are typically in the range of 0.13–0.32 (El-Fadel et al. 1999). The waste sample in Fig. 7(a) showing MSW consisting of clay soil with pieces of plastic and paper also corroborates that the likely settlement mechanism during normal landfill operations at this facility is mechanical creep.

The mechanical creep and biocompression analyses indicate that rapid settlement is a function of multiple processes. Thermal degradation, which involves the burning or pyrolysis of MSW to form charlike residuals [Fig. 7(b)], is another process that can contribute to the rapid settlement. Thermogravimetric analyses (TGAs) performed to evaluate the energy value of biomass for refuse-derived fuel applications provide a range of temperatures for MSW to thermally decompose. For example, Sørum et al. (2001)

pyrolyzed the cellulosic fraction and plastic components of MSW and showed that the major weight losses of the cellulosic matter occurred between 250 and 400°C. The thermal degradation of polystyrene, polypropylene, low-density polyethylene, and high-density polyethylene occur between 350 and 500°C. Williams and Besler (1996) investigated the thermal decomposition of cellulose and hemicellulose and established that thermal decomposition of hemicellulose begins at 250°C, while cellulose decomposition starts at 325°C.

The TGAs used to assess MSW as a source of biomass fuel indicate that temperatures above 250°C are necessary for MSW to undergo pyrolysis into charred ash. Subsurface temperatures sufficient to initiate pyrolysis have been measured in MSW landfills. For example, temperatures in MSW landfills have been reported from 200 to 300°C and as high as 700°C (Ettala et al. 1996; Lönnermark et al. 2008; Ruokojärvi et al. 1995; Bergström and Björner 1992). The charred waste in Fig. 7(b) suggests that thermal degradation does contribute to the accelerated settlement, though waste temperatures were not measured at this site because of elevated gas and leachate pressures prevented drilling into Cell 5. In summary, the main mechanisms leading to the rapid settlement illustrated in Figs. 8 and 12 are likely moisture loss and thermal degradation.

Carbon Monoxide

Carbon monoxide is typically not detected or is found at low concentrations, e.g., <100 ppmv, in normal operating anaerobic and bioreactor landfills (U.S. Fire Administration 2002; Christensen et al. 1996, 2011; Rettenberger and Stegmann 1996). Powell et al. (2006) monitored an aerobic landfill and detected average CO levels of 245 ppmv with a maximum concentration of 1,200 ppmv. Waste temperatures remained below 76°C during the study, so Powell et al. (2006) concluded that CO was produced as a result of biological degradation of the waste under limited oxygen conditions. Evidence of biological sources of CO have been reported in laboratory experiments (Thauer 1998; Diekert et al. 1984; Bott and Thauer 1987). For example, methanogenic archaea can utilize CO as a nutrient to produce methane (Thauer 1998). Diekert et al. (1984) found that acetogenic bacteria can mediate the formation of CO from CO_2. Bott and Thauer (1987) demonstrated that cell suspensions of methanogens incubated in serum bottles at 37 and 65°C formed up to 15,000 ppmv (1.5% v/v) CO in presence of a mixture 80% v/v hydrogen and 20% v/v CO_2. These studies suggest that CO can be generated from a biological source in laboratory-controlled conditions. However, ETLEs are complex and dynamic environments, in which it may prove difficult for appropriate conditions to be present, especially as temperatures increase above 75°C.

The presence of CO in MSW landfills has been associated with subsurface combustion (Ettala et al. 1996; Frid et al. 2010; Bates 2004; Martin et al. 2013; Stearns and Petoyan 1984; Sperling and Henderson 2001). Carbon monoxide is generated during smoldering combustion when insufficient oxygen is present to allow complete combustion and generation of water vapor and CO_2 (Shafizadeh and Bradbury 1979; Quintiere et al. 1982; Pitts et al. 1994; Ohlemiller 1995). The stoichiometric CO concentration determined from the reaction in Eq. (3) is approximately 54,500 ppmv, which represents an upper bound estimate. According to Quintiere et al. (1982), smoldering combustion results in CO of 100 to 10,000 ppmv. In comparison, the average and maximum CO concentrations in this case study are 5,300 and 14,400 ppmv, respectively [Fig. 11(a)]. The stoichiometric value is higher than the average measured concentration at this facility because the reaction in Eq. (3) does not account for possible combustion inefficiencies that may be present in a landfill, e.g., temperatures lower than the adiabatic flame temperature and conversion of moisture in the MSW to steam.

Hydrogen

Acetogenesis is the biological process that bridges the acidogenesis and methanogenesis stages in anaerobic decomposition (Barlaz et al. 2010). Acetogenic microorganisms break down the end of acidogenesis into acetic acid, CO_2, and hydrogen. Next, methanogenic microorganisms convert these products into methane and CO_2. Methanogenic activities are reduced at temperatures above 55°C and generally inhibited at temperatures exceeding 65°C (Bareither et al. 2013). However, acetogens have a higher temperature tolerance than methanogens. For example, Lee et al. (2008) monitored the performance of anaerobic digesters fed with artificial kitchen waste that operated at thermophilic temperatures. Although methane conversion efficiencies were high at 55°C, they decreased with increasing temperature and methane was not produced over 73°C. Lee et al. (2008) characterized the microbial population and found that methanogens were dominant below 65°C and acetogens were dominant over 73°C. Similarly, Ueno et al. (2007) reports that fermentative hydrogen accumulation from pulverized garbage and shredded paper waste dominated over methane production in a digester seeded with thermophilic fermentative bacteria and operated at 60°C. As a result, hydrogen, CO_2, and acetic acid may build up due to ongoing acetogenesis processes because methanogenesis is reduced or inhibited at temperatures above approximately 65°C. It is feasible that heat generated from the elevated temperature region is transferred via conduction and convection to surrounding wastes, thereby increasing waste temperatures such that acetogenesis is the dominant biological process and hydrogen gas is produced. This mechanism suggests that the hydrogen gas develops prior to the elevated temperature event arrival and proceeds until biological activity is inhibited at temperatures above 80°C (Haug 1997; Hogland and Marques 2003).

Another possibility for hydrogen gas production is hydrolysis and/or corrosion of metallic aluminum and iron. The presence of aluminum dross and salt cake in landfills has resulted in significant temperature increase and hydrogen generation (Calder and Stark 2010; Jafari et al. 2014b). For example, Stark et al. (2012) found hydrogen levels increased to 40% v/v after an APW reaction was initiated. However, this reaction depends on certain wastes to be disposed at the site. For the case study described herein, a search of weight receipts did not yield substantial evidence of aluminum or iron wastes.

Copping et al. (2007) reported that landfill gas contained hydrogen levels in excess of 20% v/v from regions where water was slowly introduced into an elevated temperature area. Copping et al. (2007) unfortunately did not provide the mechanism(s) for elevated hydrogen levels. One possible explanation is pyrolysis, i.e., the chemical breakdown of a substance into lower weight molecules in the presence of elevated temperatures and absence of oxygen (Fire 1996). Pyrolysis of cellulosic materials can cause the generation of CO, CO_2, and hydrogen, but typically not until temperatures are 250–500°C (Kubler 1982; Pitts et al. 1994; Shafizadeh and Bradbury 1979). In particular, Shafizadeh and Bradbury (1979) stated that low-temperature pyrolysis (torrefaction) of cellulosic materials, such as wood, paper, and other fibrous products, at temperatures less than 300°C yields products of char and a gas mixture containing CO and CO_2. Typical CO and CO_2 concentrations are 0.25 and 0.75 kg, respectively, for 1 kg of total gas produced (Neves et al. 2011). At temperatures above 300°C, the cellulose is decomposed by an alternative pathway, and the major evolved product is liquid, gases (CO, CO_2, hydrogen), and char (Antal et al. 1980). The evolution of hydrogen gas during pyrolysis first appears at low concentrations at 600°C, and generally reaches 20% v/v of gas composition by 700°C (Neves et al. 2011).

Alternatively, hydrogen gas can be generated at lower pyrolysis temperatures (200–250°C) by the water-gas shift reaction [Eq. (5)]. In this moderately exothermic reaction, CO reacts with steam to form CO_2 and hydrogen gases (Demirel and Azcan 2012). The conversion of CO to hydrogen is thermodynamically favored at low pyrolysis temperatures, but the reaction rate is kinetically favored at higher temperatures (~700°C). In other words, the process is temperature dependent, which means CO is converted to hydrogen at 250°C but the conversion rate is slow. Similar to the water-gas shift reaction, the water-gas reaction is an endothermic and irreversible reaction that converts carbon and steam into a synthesis gas. The rate of the reaction in Eq. (5) is dependent on the nature of the carbonaceous solid as well as the temperature and steam concentration

$$CO + H_2O \rightarrow CO_2 + H_2 \qquad \Delta H = -41.1 \text{ kJ/mol} \tag{5}$$

The lack of waste temperatures correlated to gas composition in the elevated temperature region and surrounding wastes precludes the capability of identifying a single mechanism causing the observed hydrogen gas. Thus, several mechanisms were presented to explain the presence of elevated hydrogen concentrations. To summarize, heat emanating from the elevated temperature region can increase waste temperatures above the threshold of methanogenesis and permit acetogenesis, where hydrogen, CO_2, and acetic acid are produced. Pyrolysis of MSW can produce CO concentrations of approximately 35% v/v (Neves et al. 2011). Steam produced from dehydration of MSW and CO can react via the water-gas shift reaction to form hydrogen gas. Pyrolysis can also generate hydrogen gas at temperatures greater than 300°C. In both pyrolysis and water-gas shift reactions, the temperature threshold and reaction rates can be affected by catalysts present in MSW (such as zinc, copper, and nickel metals).

Summary

Elevated temperatures above the NSPS threshold can significantly affect the behavior and operation of a MSW landfill. If not addressed in an expedient manner, ETLEs can result in damage to landfill infrastructure, e.g., gas extraction, leachate collection, and bottom liner system; slope instability; and environmental conditions that adversely affect the health and welfare of the local community. This paper identifies the main indicators of elevated temperatures and arranges them in the following chronological sequence: (1) changes in landfill gas composition, (2) elevated waste and gas temperatures, (3) elevated gas and leachate pressures, (4) increased leachate migration, (5) slope movement, and (6) rapid and unusual settlement. The case study presented herein yielded the following recommendations:

- Gas wellhead temperatures should be correlated with downhole temperatures because they are more reliable, approximate the maximum temperatures, identify depth of interest, and show time-lapse changes. Wellhead temperatures typically underpredict waste temperatures because gases are extracted over the full height and radius of influence of the well. The observed underprediction varies among different landfills, with this case study reporting a difference of approximately 20°C.
- During the expansion and/or migration of ETLEs, landfill gas quickly changes from predominantly methane (50–60% v/v) and CO_2 (40–55% v/v) to a composition of CO_2 (60–80% v/v), hydrogen (10–35% v/v), and CO (>1,500 ppmv).
- The settlement rates estimated for anaerobic biodegradation and elevated temperatures (pyrolysis and combustion), are ~0.5 m/year (0.6%/year) and ~4.6 m/year (5.7%/year), respectively, and can result in formation of a settlement bowl.
- Biological and chemical processes are proposed herein to explain changes in gas composition and settlement. The main mechanisms for rapid settlement are a combination of moisture loss and thermal degradation. Smoldering combustion and pyrolysis explain the generation of CO and thermal degradation of MSW, respectively. Acetogenesis, water-gas shift reaction, and pyrolysis are proposed to help explain elevated hydrogen production. However, further research is necessary to determine the exact cause of hydrogen generation in MSW landfills when subjected to elevated temperatures.

Acknowledgments

The authors would like to acknowledge Andony Landivar and Mario Hernandez for assistance in data reduction and preparation of the manuscript. The contents and views in this paper are those of the authors and do not necessarily reflect those of any landfill owner or operator, homeowners, consultants, regulatory agency or personnel, or anyone else involved in case studies referenced. In particular, the contents of this paper are the personal opinions of the authors and may not reflect the opinions, conclusions, policies or procedures of the California Environmental Protection Agency or CalRecycle.

References

Antal, M. J., Friedman, H. L., and Rogers, F. E. (1980). "Kinetics of cellulose pyrolysis in nitrogen and steam." *Combust. Sci. Tech.*, 21(3–4), 141–152.

Anthony, E. J., Jia, L., Caris, M., Preto, F., and Burwell, S. (1999). "An examination of the exothermic nature of fluidized bed combustion (FBC) residues." *Waste Manage.*, 19(4), 293–305.

Bareither, C. A., Benson, C. H., and Edil, T. B. (2012a). "Compression of municipal solid waste in bioreactor landfills: Mechanical creep and biocompression." *J. Geotech. Geoenviron. Eng.*, 10.1061/(ASCE)GT.1943-5606.0000835, 1007–1021.

Bareither, C. A., Breitmeyer, R. J., Benson, C. H., Barlaz, M. A., and Edil, T. B. (2012b). "Deer track bioreactor experiment: Field-scale evaluation of municipal solid waste bioreactor performance." *J. Geotech. Geoenviron. Eng.*, 10.1061/(ASCE)GT.1943-5606.0000636, 658–670.

Bareither, C. A., Wolfe, G. L., McMahon, K. D., and Benson, C. H. (2013). "Microbial diversity and dynamics during methane production from municipal solid waste." *Waste Manage.*, 33(10), 1982–1992.

Barlaz, M. A., Staley, B. F., and de los Reyes, F. L. (2010). "Anaerobic biodegradation of solid waste." *Environmental microbiology*, R. Mitchell and J.-D. Gu, eds., 2nd Ed., Wiley-Blackwell, Hoboken, NJ, 281–299.

Bates, M. (2004). "Managing landfill site fires in Northamptonshire." Northamptonshire County Council, Northampton, U.K.

Bergström, J., and Björner, B. (1992). "Dioxins and fires in waste storage." *Rep. No. 68*, REFORSK Foundation, Malmö, Sweden.

Bjarngard, A., and Edgers, L. (1990). "Settlement of municipal solid waste landfills." *Proc., 13th Annual Madison Waste Conf.*, Univ. of Wisconsin-Madison, Madison, WI, 192–205.

Blight, G. (2008). "Slope failures in municipal solid waste dumps and landfills: A review." *Waste Manage. Res.*, 26(5), 448–463.

Bogner, J., Rose, C., Vogt, M., and Gartman, D. (1988). "Understanding landfill gas generation and migration." *Proc., 11th Annual Int. Landfill Gas Symp.*, Government Refuse Collection and Disposal Association, Silver Spring, MD, 225–242.

Bott, M., and Thauer, R. K. (1987). "Proton-motive-force-driven formation of CO from CO_2 and H_2 in methanogenic bacteria." *Eur. J. Biochem.*, 168(2), 407–412.

Buah, W. K., Cuncliffe, A. M., and Williams, P. T. (2007). "Characterization of products from the pyrolysis of municipal solid waste." *Process Saf. Environ.*, 85(5), 450–457.

Calder, G. V., and Stark, T. D. (2010). "Aluminum reactions and problems in municipal solid waste landfills." *Pract. Period. Hazard. Toxic Radioact. Waste Manage.*, 10.1061/(ASCE)HZ.1944-8376.0000045, 258–265.

Cecchi, F., Pavan, P., Musacco, A., Mata Álvarez, J., and Vallini, G. (1993). "Digesting the organic fraction of municipal solid waste: Moving from mesophilic (37°C) to thermophilic (55°C) conditions." *Waste Manage. Res.*, 11(5), 403–414.

Christensen, T. H., Cossu, R., and Stegmann, R., eds. (1996). *Landfilling of waste: Biogas*, E & FN Spon, London.

Christensen, T. H., Manfredi, S., and Knox, K. (2011). "Landfilling: Reactor landfills." *Solid waste technology and management*, T. H. Christensen, ed., Blackwell, Chichester, U.K., 772–787.

Chrysikou, L., Gemenetzis, P., Kouras, A., Manoli, E., Terzi, E., and Samara, C. (2008). "Distribution of persistent organic pollutants, polycyclic aromatic hydrocarbons and trace elements in soil and vegetation following a large scale landfill fire in northern Greece." *Environ. Int.*, 34(2), 210–225.

Copping, S., Quinn, C., and Gregory, R. (2007). "Review and investigation of deep-seated fires within landfill sites." *Science Rep. No. SC010066*, Environment Agency, Bristol, U.K.

Crutcher, A. J., Rovers, F. A., and McBean, E. A. (1982). "Temperature as an indicator of landfill behavior." *Water Air Soil Pollut.*, 17(2), 213–223.

De Haan, J. D. (2006). *Kirk's fire investigation*, 6th Ed., Prentice Hall, Upper Saddle River, NJ.

Demirel, E., and Azcan, N. (2012). "Thermodynamic modeling of water-gas shift reaction in supercritical water." *Proc., World Congress on Engineering and Computer Science*, S. I. Ao, C. Douglas, W. S. Grundfest, and J. Burgstone, eds., International Association of Engineers, Hong Kong, 804–807.

Diekert, G., Hansch, M., and Conrad, R. (1984). "Acetate synthesis from 2 CO_2 in acetogenic bacteria: Is carbon monoxide an intermediate?" *Arch. Microbiol.*, 138(3), 224–228.

DMWM (Division of Materials and Waste Management). (2011). "Subsurface heating events at solid waste and construction and demolition debris landfills: Best management practices." *Guidance Document #1009*, Ohio Environmental Protection Agency, Columbus, OH.

El-Fadel, M., Findikakis, A. N., and Leckie, J. O. (1997). "Environmental impacts of solid waste landfilling." *J. Environ. Manage.*, 50(1), 1–25.

El-Fadel, M., Shazbak, S., Saliby, E., and Leckie, J. O. (1999). "Comparative assessment of settlement models for municipal solid waste landfill applications." *Waste Manage. Res.*, 17(5), 347–368.

Emcon Associates. (1981). "State-of-the-art of methane gas enhancement in landfills." *ANL/CNSV-23*, Argonne National Laboratory, Argonne, IL.

Ettala, M., Rahkonen, P., Rossi, E., Mangs, J., and Keski-Rahkonen, O. (1996). "Landfill fires in Finland." *Waste Manage. Res.*, 14(4), 377–384.

Eun, J., Tinjum, J. M., Benson, C. H., and Edil, T. B. (2014). "Volatile organic compound (VOC) transport through a composite liner with co-extruded geomembrane containing ethylene vinyl-alcohol (EVOH)." *Geo-Congress 2014 Technical Papers: Geo-Characterization and Modeling for Sustainability*, M. Abu-Farsakh, X. Yu, and L. R. Hoyos, eds., ASCE, Reston, VA, 1960–1969.

Farquhar, G. J., and Rovers, F. A. (1973). "Gas production during refuse decomposition." *Water Air Soil Pollut.*, 2(4), 483–495.

Fire, F. L. (1996). "Fire and pyrolysis." *The common sense approach to hazardous materials*, 2nd Ed., PennWell, Tulsa, OK, 105–123.

Fluke. (2010). "51 & 52 Series II: Users manual." Everett, WA.

Frid, V., et al. (2010). "Geophysical-geochemical investigation of fire-prone landfills." *Environ. Earth Sci.*, 60(4), 787–798.

Hanson, J. L., Yesiller, N., and Oettle, N. (2010). "Spatial and temporal temperature distributions in municipal solid waste landfills." *J. Environ. Eng.*, 10.1061/(ASCE)EE.1943-7870.0000202, 804–814.

Hartz, K. E., Klink, R. E., and Ham, R. K. (1982). "Temperature effects: Methane generation from landfill samples." *J. Environ. Eng.*, 108(4), 629–638.

Haug, R. T. (1997). "Feedstocks, conditioning, and fire prevention." *BioCycle*, 38(4), 68–70.

Hendron, D. M., Fernandez, G., Prommer, P. J., Giroud, J. P., and Orozco, L. F. (1999). "Investigation of the cause of the 27 September 1997 slope failure at the Doña Juana landfill." *Proc., Sardinia '99, 7th Int. Waste Management and Landfill Symp.*, Environmental Sanitary Engineering Centre, Cagliari, Italy, 545–554.

Hogland, W., and Marques, M. (2003). "Physical, biological and chemical processes during storage and spontaneous combustion of waste fuel." *Resour. Conserv. Recycl.*, 40(1), 53–69.

Hossain, M. S., and Gabr, M. A. (2005). "Prediction of municipal solid waste landfill settlement with leachate recirculation." *Proc., Geo-Frontiers 2005*, A. Alshawabkeh, et al., eds., ASCE, Reston, VA, 1–14.

Houi, D., Paul, E., and Couturier, C. (1997). "Heat and mass transfer in landfills and biogas recovery." *Proc., Sardinia '97, 6th Int. Waste Management and Landfill Symp.*, Environmental Sanitary Engineering Centre, Cagliari, Italy, 101–108.

Hudgins, M., and Harper, S. (1999). "Operational characteristics of two aerobic landfill systems." *Proc., Sardinia '99, 7th Int. Waste Management and Landfill Symp.*, Environmental Sanitary Engineering Centre, Cagliari, Italy, 1–9.

Huggett, C. (1980). "Estimation of rate of heat release by means of oxygen consumption measurements." *Fire Mater.*, 4(2), 61–65.

Ishigaki, T., Yamada, M., Nagamori, M., Ono, Y., and Inoue, Y. (2005). "Estimation of methane emission from whole waste landfill site using correlation between flux and ground temperature." *Environ. Geol.*, 48(7), 845–853.

Jafari, N. H., Stark, T. D., and Merry, S. M. (2013). "The 10 July 2000 Payatas landfill slope failure." *Int. J. Geoeng. Case Histories*, 2(3), 208–228.

Jafari, N. H., Stark, T. D., and Roper, R. (2014a). "Classification and reactivity of aluminum production waste." *J. Hazard. Toxic Radioact. Waste*, 10.1061/(ASCE)HZ.2153-5515.0000223, 04014018.

Jafari, N. H., Stark, T. D., and Rowe, K. (2014b). "Service life of HDPE geomembranes subjected to elevated temperatures." *J. Hazard. Toxic Radioact. Waste*, 10.1061/(ASCE)HZ.2153-5515.0000188, 16–26.

Kasali, G. B., and Senior, E. (1989). "Effects of temperature and moisture on the anaerobic digestion of refuse." *J. Chem. Tech. Biotechnol.*, 44(1), 31–41.

Kerfoot, H. B. (1993). "Landfill gas effects on groundwater samples at a municipal solid waste facility." *Proc., Sardinia '93, 4th Int. Landfill Symp.*, T. H. Christensen, R. Cossu, and R. Stegmann, eds., Environmental Sanitary Engineering Centre, Cagliari, Italy, 1141–1154.

Kjeldsen, P., and Fischer, E. V. (1995). "Landfill gas migration—Field investigations at Skellingsted Landfill, Denmark." *Waste Manage. Res.*, 13(5), 467–484.

Klein, R., Baumann, T., Kahapka, E., and Niessner, R. (2001). "Temperature development in a modern municipal solid waste incineration (MSWI) bottom ash landfill with regard to sustainable waste management." *J. Hazard. Mater.*, 83(3), 265–280.

Klein, R., Nestle, N., Niessner, R., and Baumann, T. (2003). "Numerical modelling of the generation and transport of heat in a bottom ash monofill." *J. Hazard. Mater.*, 100(1–3), 147–162.

Koelsch, F., Fricke, K., Mahler, C., and Damanhuri, E. (2005). "Stability of landfills—The Bandung dumpsite disaster." *Proc., Sardinia 2005, 10th Int. Waste Management and Landfill Symp.*, R. Cossu and R. Stegmann, eds., Environmental Sanitary Engineering Centre, Cagliari, Italy.

Koerner, R. M., and Soong, T.-Y. (2000). "Leachate in landfills: The stability issues." *Geotext. Geomembr.*, 18(5), 293–309.

Kubler, H. (1982). "Heat release in thermally disintegrating wood." *Wood Fiber*, 14(3), 166–177.

LANDTEC. (2010). "GEM2000 Plus operation manual." Colton, CA.

Lee, M. Y., Cheon, J. H., Hidaka, T., and Tsuno, H. (2008). "The performance and microbial diversity of temperature-phased hyperthermophilic and thermophilic anaerobic digestion system fed with organic waste." *Water Sci. Technol.*, 57(2), 283–289.

Lefebvre, X., Lanini, S., and Houi, D. (2000). "The role of aerobic activity on refuse temperature rise. I: Landfill experimental study." *Waste Manage. Res.*, 18(5), 444–452.

Lewicki, R. (1999). "Early detection and prevention of landfill fires." *Proc., Sardinia '99, 7th Int. Waste Management and Landfill Symp.*, Environmental Sanitary Engineering Centre, Cagliari, Italy.

Lin, K.-S., Wang, H. P., Liu, S.-H., Chang, N.-B., Huang, Y.-J., and Wang, H.-C. (1999). "Pyrolysis kinetics of refuse-derived fuel." *Fuel Process. Technol.*, 60(2), 103–110.

Lönnermark, A., Blomquist, P., and Marklund, S. (2008). "Emission from simulated deep-seated fires in domestic waste." *Chemosphere*, 70(4), 626–639.

Martin, J. W., Stark, T. D., Thalhamer, T., Gerbasi-Graf, G. T., and Gortner, R. E. (2013). "Detection of aluminum waste reactions and waste fires." *J. Hazard. Toxic Radioact. Waste*, 10.1061/(ASCE)HZ.2153-5515.0000171, 164–174.

Mata Álvarez, J., and Martínez Viturtia, A. (1986). "Laboratory simulation of municipal solid waste fermentation with leachate recycle." *J. Chem. Tech. Biotechnol.*, 36(12), 547–556.

McBean, E. A., Rovers, F. A., and Farquhar, G. J. (1995). *Solid waste landfill engineering and design*, Prentice Hall, Englewood Cliffs, NJ.

McWatters, R., and Rowe, R. (2015). "Permeation of volatile organic compounds through EVOH thin film membranes and coextruded LLDPE/EVOH/LLDPE geomembranes." *J. Geotech. Geoenviron. Eng.*, 10.1061/(ASCE)GT.1943-5606.0001209, 04014091.

Meraz, L., and Domínguez, A. (1998). "A calorimetric description of the digestion of organic matter in landfills." *Chem. Educator*, 3(6), 1–6.

Merry, S. M., Fritz, W. U., Budhu, M., and Jesionek, K. (2005). "Effect of gas on pore pressures in wet landfills." *J. Geotech. Geoenviron. Eng.*, 10.1061/(ASCE)1090-0241(2006)132:5(553), 553–561.

Merz, R. C., and Stone, R. (1970). "Special studies of a sanitary landfill." *EPA-SW-8RG-70*, Bureau of Solid Waste Management, U.S. EPA, Rockville, MD.

Nammari, D. R., Hogland, W., Marques, M., Nimmermark, S., and Moutavtchi, V. (2004). "Emission from uncontrolled fire in municipal solid waste bales." *Waste Manage.*, 24(1), 9–18.

Nastev, M., Therrien, R., Lefebvre, R., and Gélinas, P. (2001). "Gas production and migration in landfills and geological materials." *J. Contam. Hydrol.*, 52(1–4), 187–211.

Neves, D., Thunman, H., Matos, A., Tarelho, L., and Gómez Barea, A. (2011). "Characterization and prediction of biomass pyrolysis products." *Prog. Energy Combust. Sci.*, 37(5), 611–630.

Nikolaou, K. (2008). "Environmental management and landfill fire accidents." *J. Environ. Prot. Ecol.*, 9(4), 830–834.

Ohlemiller, T. J. (1995). "Smoldering combustion." *SFPE handbook of fire protection engineering*, 2nd Ed., P. M. DiNenno, et al. eds., National Fire Protection Association, Quincy, MA, 2-171–2-179.

Øygard, J. K., Måge, A., Gjengedal, E., and Svane, T. (2005). "Effect of an uncontrolled fire and the subsequent fire fight on the chemical composition of landfill leachate." *Waste Manage.*, 25(7), 712–718.

Pfeffer, J. T. (1974). "Temperature effects on anaerobic fermentation of domestic refuse." *Biotechnol. Bioeng.*, 16(6), 771–787.

Pitts, W. M. (2007). "Ignition of cellulosic fuels by heated and radiative surfaces." *NIST Technical Note 1482*, National Institute of Standards and Technology, Gaithersburg, MD.

Pitts, W. M., Johnsson, E. L., and Bryner, N. O. (1994). "Carbon monoxide formation in fires by high-temperature anaerobic wood pyrolysis." *Proc., 25th Symp. on Combustion*, Combustion Institute, Pittsburgh, 1455–1462.

Powell, J., Jain, P., Kim, H., Townsend, T., and Reinhart, D. (2006). "Changes in landfill gas quality as a result of controlled air injection." *Environ. Sci. Technol.*, 40(3), 1029–1034.

Quintiere, J. G., Birky, M., Macdonald, F., and Smith, G. (1982). "An analysis of smoldering fires in closed compartments and their hazard due to carbon monoxide." *Fire Mater.*, 6(3–4), 99–110.

Rampling, T. W., and Hickey, T. J. (1988). "The laboratory characterization of refuse derived fuel." *Warren Laboratory, Rep. No. LR643*, U.K. Dept. of Trade and Industry, London.

Rettenberger, G., and Stegmann, R. (1996). "Landfill gas components." *Landfilling of waste: Biogas*, T. H. Christensen, R. Cossu, and R. Stegmann, eds., E & FN Spon, London, 51–58.

Riquier, L., Guerbois, M., Budka, A., Hebe, I., and Riviere, S. (2003). "Underground fire characterisation in landfills: Investigation methods." *Proc., Sardinia 2003, 9th Int. Waste Management and Landfill Symp.*, T. H. Christensen, R. Cossu, and R. Stegmann, eds. Environmental Sanitary Engineering Centre, Cagliari, Italy.

Riviere, S., Goumand, J. C., Guerbois, M., and Hebe, I. (2003). "Characterisation of underground fires in landfills using geophysical methods: A case study." *Proc., Sardinia 2003, 9th Int. Waste Management and Landfill Symp.*, T. H. Christensen, R. Cossu, and R. Stegmann, eds., Environmental Sanitary Engineering Centre, Cagliari, Italy.

Ruokojärvi, P., Ruuskanen, J., Ettala, M., Rahkonen, P., and Tarhanen, J. (1995). "Formation of polyaromatic hydrocarbons and polychlorinated organic compounds in municipal waste landfill fires." *Chemosphere*, 31(8), 3899–3908.

Shafizadeh, F., and Bradbury, A. G. W. (1979). "Thermal degradation of cellulose in air and nitrogen at low temperatures." *J. Appl. Polym. Sci.*, 23(5), 1431–1442.

Shaw Environmental. (2008). "Area 3 work plan: Expanded heat and pressure investigation." Illinois Environmental Protection Agency, Springfield, IL.

Sørum, L., Grønli, M. G., and Hustan, J. E. (2001). "Pyrolysis characteristics and kinetics of municipal solid wastes." *Fuel*, 80(9), 1217–1227.

Sperling, T., and Henderson, J. P. (2001). "Understanding and controlling landfill fires." *Proc., 6th Annual Landfill Symp.*, Solid Waste Association of North America, Silver Spring, MD.

Stark, T. D., Akhtar, K., and Hussain, M. (2010). "Stability analyses for landfills experiencing elevated temperatures." *Proc., GeoFlorida 2010: Advances in Analysis, Modeling and Design*, D. O. Fratta, A. J. Puppala, and B. Muhunthan, eds., ASCE Geo-Institute, Reston, VA, 3110–3119.

Stark, T. D., Martin, J. W., Gerbasi, G. T., Thalhamer, T., and Gortner, R. E. (2012). "Aluminum waste reaction indicators in a municipal solid waste landfill." *J. Geotech. Geoenviron. Eng.*, 10.1061/(ASCE)GT.1943-5606.0000581, 252–261.

Stearns, R. P., and Petoyan, G. S. (1984). "Identifying and controlling landfill fires." *Waste Manage. Res.*, 2(1), 303–309.

Szczygielski, T. (2007). "Fire in the hole: Aluminum dross in landfills." *J. Natl. Resour. Environ. L.*, 22(2), 159–174.

Thauer, R. K. (1998). "Biochemistry of methanogenesis: A tribute to Marjory Stephenson." *Microbiology*, 144(9), 2377–2406.

Ueno, Y., Fukui, H., and Goto, M. (2007). "Operation of a two-stage fermentation process producing hydrogen and methane from organic waste." *Environ. Sci. Technol.*, 41(4), 1413–1419.

USACE (U.S. Army Corps of Engineers). (2008). "Landfill off-gas collection and treatment systems." *EM 1110-1-4016*, Washington, DC.

U.S. Fire Administration. (2002). "Landfill fires: Their magnitude, characteristics, and mitigation." *Miscellaneous No.: FA-225*, Federal Emergency Management Agency, Emmitsburg, MD.

Wappett, H. L., and Zornberg, J. G. (2006). "Full scale monitoring for assessment of exothermal reactions in waste tires." *Recycled Materials Resource Center Project No. 27: Final Rep.*, Federal Highway Administration, Washington, DC.

Williams, G. M., and Aitkenhead, N. (1991). "Lessons from Loscoe: The uncontrolled migration of landfill gas." *Q. J. Eng. Geol.*, 24(2), 191–207.

Williams, P. T., and Besler, S. (1993). “The pyrolysis of rice husks in a thermogravimetric analyser and static batch reactor.” *Fuel*, 72(2), 151–159.

Williams, P. T., and Besler, S. (1996). “The influence of temperature and heating rate on the slow pyrolysis of biomass.” *Renew. Energy*, 7(3), 233–250.

Wittmann, S. G. (1985). “Landfill gas migration: Early warning signs, monitoring techniques and migration control systems.” *Proc., 23rd Annual Int. Seminar, Equipment, Services, and Systems Show*, Garbage Refuse Collection and Disposal Association, Silver Spring, MD, 317–328.

Yesiller, N., Hanson, J., and Liu, W. (2005). “Heat generation in municipal solid waste landfills.” *J. Geotech. Geoenviron. Eng.*, 10.1061/(ASCE)1090-0241(2005)131:11(1330), 1330–1344.

Young, A. (1992). “Application of computer modelling to landfill processes.” *Rep. No. CWM 039/92*, U.K. Dept. of the Environment, London.

Zerlottin, M., Refosco, D., Della Zassa, M., Biasin, A., and Canu, P. (2013). “Self-heating of dried wastewater sludge.” *Waste Manage.*, 33(1), 129–137.

Zinder, S. H. (1993). “Physiological ecology of methanogens.” *Methanogenesis: Ecology, physiology, biochemistry and genetics*, J. G. Ferry, ed., Chapman & Hall, New York, 128–206.